Chemical Research in Toxicology

pubs.acs.org/crt

Article

Mycotoxin Altertoxin II Induces Lipid Peroxidation Connecting Mitochondrial Stress Response to NF-κB Inhibition in THP-1 Macrophages

Giorgia Del Favero,* Julia Hohenbichler, Raphaela Maria Mayer, Michael Rychlik, and Doris Marko

Cite This: *Chem. Res. Toxicol.* 2020, 33, 492−504

Read Online

ACCESS | Metrics & More | Article Recommendations

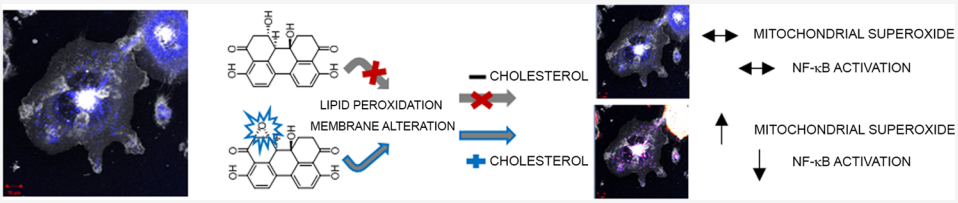

ABSTRACT: Prolonged exposure to mycotoxins, even in subtoxic concentrations, might contribute to modulate pro- or anti-inflammatory cascades and ultimately have long-term consequences on our health. In line, there is an increasing need to describe and comprehend the potential immunomodulatory effects of toxins that can be produced from fungi proliferating even in a domestic environment like, for instance, *Alternaria alternata*. Taking this as a starting point, we investigated the effects of one of the most potent genotoxic compounds produced by this fungi type, namely altertoxin II (ATXII) on THP-1 macrophages. In noncytotoxic concentrations (0.1−1 μM), ATXII inhibited the activation of the transcription factor NF-κB, and this event was accompanied by significant mitochondrial superoxide production (1 μM ATXII). Both responses seemed dependent on membrane structure and morphology since they were modulated by the coincubation with the cholesterol complexing agent methyl-β-cyclodextrin (MβCD, 10−50 μM). Moreover, toxicity of ATXII was enhanced by cholesterol load (cholesterol-MβCD). The mycotoxin induced also lipid peroxidation (1−10 μM, ATXII) possibly streaming down at the mitochondrial level and suppressing NF-κB activation in THP-1 macrophages.

INTRODUCTION

The heterogeneity of mycotoxin structures is reflected by a broad spectrum of modes of action. Among these, increasing attention is given to the interaction of fungal metabolites with the immune system. Immunomodulatory potential has been described as primary or secondary mechanisms of action of several mycotoxins. This is, for instance, the case for fumonisin B1[1,2] or deoxynivalenol and related compounds.[3−6] Even though several papers have been published about the effects of the regulated compounds, where maximal limits have already been established, many questions remain unsolved with respect to the less characterized "emerging" mycotoxins. Mold exposure, also in a domestic environment, can develop into a wide variety of health issues, including severe impairment of the respiratory system.[7] The molecular events sustaining these mechanisms are the topic of continuous investigation, and research proceeds in parallel to the characterization of the toxins involved. Severe asthma with fungal sensitization (SAFS) has been related to the confirmed exposure to at least one type of fungus, including among others *Alternaria alternata*.[8] *A. alternata* fungi are known aeroallergens, and Alt A 1 is one of the major allergic proteins produced by the fungus.[9,10] In addition, the molds produce hundreds of secondary metabolites, whose immunomodulatory potential is far from being completely elucidated. Among the mycotoxins produced by *A. alternata*, alternariol (AOH) is possibly the better characterized molecule, especially with respect to immunomodulation. AOH alters macrophages cell cycle[11] and inhibits the LPS-induced pro-inflammatory cascade.[4,12]

Among the secondary metabolites of *Alternaria alternata* there are several structurally different groups of molecules. In addition to the dibenzopyrones like AOH, perylene quinone toxins have been shown to play an important role in the overall toxicity of complex *Alternaria* toxin mixtures.[13,14] This group comprises several planar molecules like altertoxin I (ATXI) or alterperylenol (ALP), as well as more reactive species bearing an epoxide group like altertoxin II (ATXII) and stemphyltoxin III (STTX III). Accordingly, the latter are more difficult to detect at the systemic level[15] albeit being characterized by considerable toxic potential. It was previously demonstrated that ATXII has strong genotoxic activity,[13,14,16,17] it can trigger oxidative stress,[18]

Received: September 15, 2019
Published: February 5, 2020

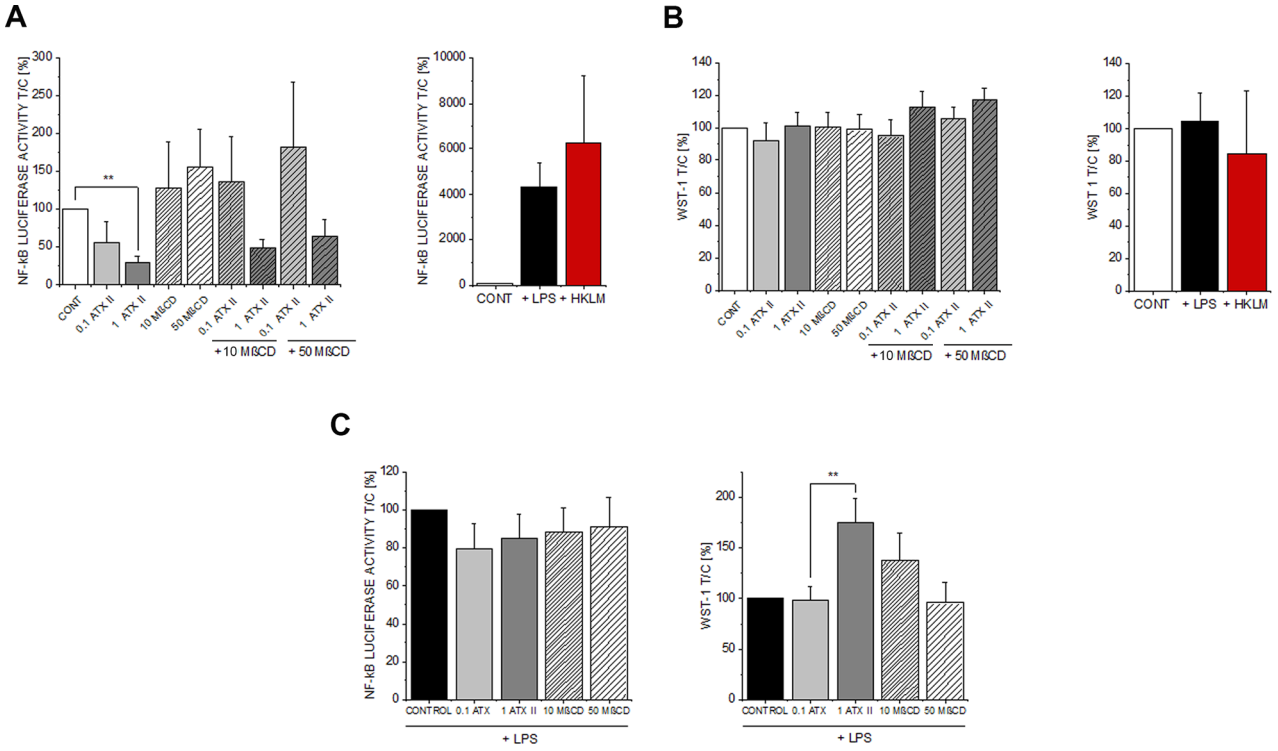

Figure 1. Effect of ATXII on the transcription factor NF-κB. (A) Concentration-dependent effect of ATXII (gray bars) and MβCD (striped bars) on the activation of NF-κB via reporter gene assay. Positive controls are provided as reference and depicted in black (LPS) and in red (HKLM, heat killed *Listeria monocytogenes*). (B) Cytotoxicity measurement by WST-1 assay. (C) Concentration-dependent effect of ATXII and MβCD on the activation of NF-κB induced by LPS (100 ng/mL, black bars) and respective WST-1 assay. Data are expressed as mean ± SE of 4 independent experiments. Direct comparison of data (A) was performed with the Mann−Whitney test $^{**}p < 0.01$ and the concentration dependent effect (C) with one-way ANOVA test followed by Fisher's test ($^{**}p < 0.01$). All concentrations are intended in [μM].

and it also has a cell type specific effect on the cell membrane biophysical properties.[19] Taking into account that LPS-induced inflammatory cascade starts through the activation of Toll-like receptor 4 (TLR4) at the membrane level and the inflammatory cascade is tightly related to oxidative stress response,[20] as well as to mitochondrial activation,[21−23] we took the crosstalk between plasma membrane and mitochondria as central processes in our study design. In line, we decided to start the characterization of the immunomodulatory potential of ATXII with the acute monocytic leukemia cell line THP-1-derived macrophages and evaluated the impact on mitochondrial morphology, superoxide production, lipid oxidative status, and membrane structure.

MATERIALS AND METHODS

Chemicals. Altertoxin II (ATXII) was purified from *Alternaria alternata* rice cultures as previously described.[13,18] Altertoxin I (ATXI) was biosynthesized and purified after inoculation of rice with *Alternaria alternata* conidia.[24] Methyl-β-cyclodextrin (MβCD), cholesterol−methyl-β-cyclodextrin (water-soluble cholesterol), and lipopolysaccharide (LPS) *Escherichia coli* O55:B5 were purchased from Sigma-Aldrich Corporation, St. Louis, US. HKLM was dissolved in sterile ddH_2O:10e10 bacteria in 50 μL of ddH_2O. For cell viability and membrane fluidity the Proliferation Reagent WST-1 (Roche Diagnostics GmbH, Mannheim, Germany) and 1-pyrenedecanoic acid (PDA, Invitrogen, Thermo Fisher Scientific, Waltham, US Life Technologies Corporation, Eugene, OR, US) were used. General cell culture reagents were purchased from Carl Roth (GmbH + Co. KG, Karlsruhe, Germany), Sigma-Aldrich Corporation (St. Louis, US), and Thermo Fisher Scientific (Waltham, US) according to availability.

Cell Culture. THP-1 monocytes (ATCC TIB202) were cultivated in RPMI 1640 medium supplemented with 10% v/v heat-inactivated fetal calf serum (FCS) and 1% v/v penicillin/streptomycin (P/S). Macrophage differentiation was obtained with phorbol-12-myristate-13-acetate (PMA, 10 ng/mL) treatment for 72 h followed by an additional 24 h in PMA free medium, as previously described.[12]

NF-κB Reporter Gene Assay. THP-1 Lucia NF-κB monocytes were subcultured in RPMI 1640 medium (Thermo-Fisher Scientific, Ref.A1049-01), containing 1% Penicillin and Streptomycin (100 U/mL) with an alternating supplementation of 100 μg/mL of zeocin and normocin formulation, respectively, to every second subculture. For the experiments THP-1 Lucia NF-κB monocytes were seeded into 96-well plates (0.1×10^6) and simultaneously incubated with ATXII (0.1−1 μM), methyl-β-cyclodextrin (10−50 μM), or combinations, solvent control (0.1% DMSO), and positive control HKLM for 20 h. For LPS-treated cells, LPS (100 ng/mL) was added 2 h after incubation of the substances and included in the treatment for the remaining 18 h. Following incubations, NF-κB reporter gene assay was performed according to the manufacturer's protocol employing Quanti-Luc (Invivogen), a coelenterazine-based luminescence reagent. NF-κB activation was measured as luciferase activity in a microplate reader. Data are mean of minimum 5 independent experiments performed in technical duplicates.

Cytotoxicity Assays. Cytotoxicity of ATXII was measured as previously described with the WST-1 assay.[25] At the end of the assays, cells were incubated with the reagent for 2 h, and absorbance was measured at 650 and 440 nm with a Cytation 3 Cell Imaging Multi-Mode Reader equipped with Gen5 Data Analysis Software (BioTek Instruments, Inc., Winooski, Vermont, USA). Data are mean of at least 4 independent experiments performed in triplicates.

Confocal and Structured Illumination Microscopy. For the immunofluorescence experiments THP-1 macrophages were incubated according to the protocol of interest, fixed with prewarmed 3.7% formaldehyde, and washed with PBS. Permeabilization was performed with 0.2% Triton X-100 followed by blocking with 2% donkey serum. Primary antibodies were diluted according to the specification of

https://dx.doi.org/10.1021/acs.chemrestox.9b00378
Chem. Res. Toxicol. 2020, 33, 492−504

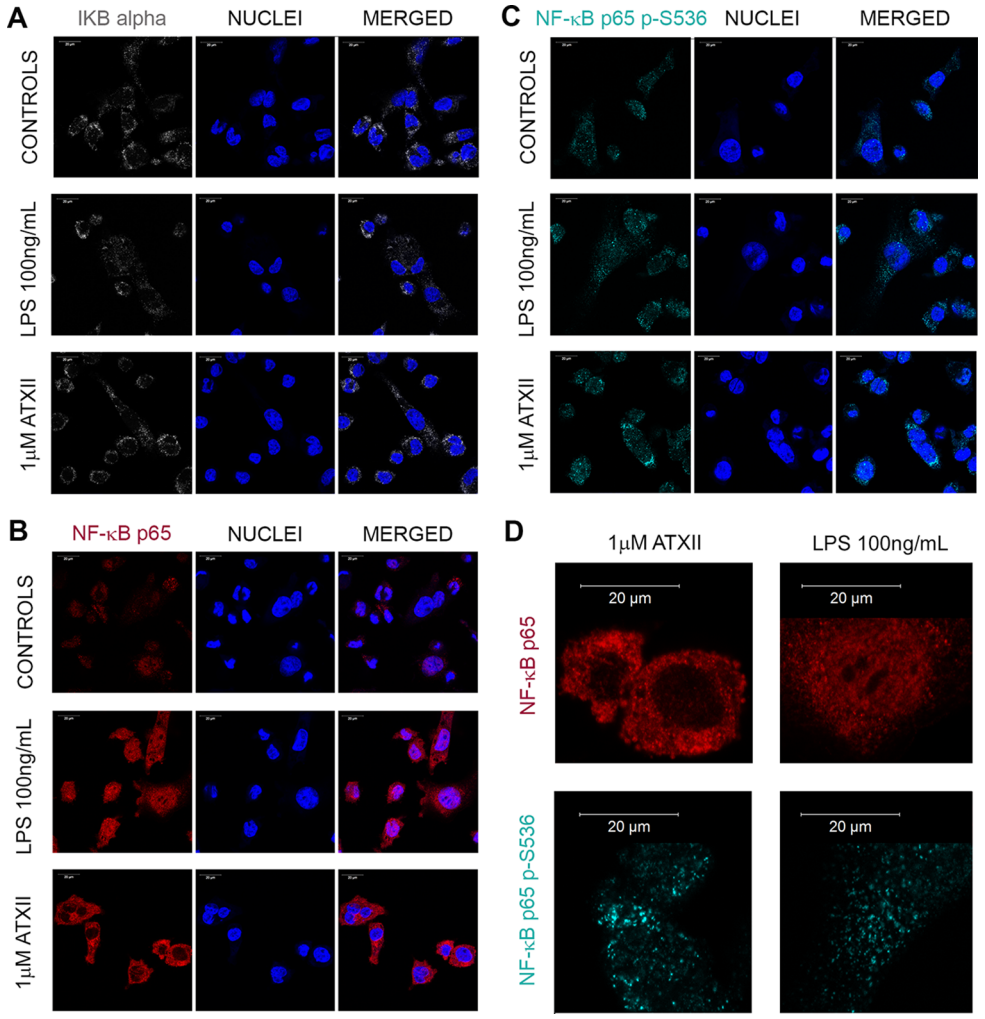

Figure 2. Representative immunolocalization of IKB alpha (gray, A), NF-κB p65 (red, B), and NF-κB p65 p-S536 (light blue, C) in control cells or after 1 h incubation with 1 μM ATXII or LPS 100 ng/mL. (D) Details of the immunolocalization of NF-κB p65 (red) and NF-κB p65 p-S536 (light blue). Cell nuclei are counterstained with DAPI (blue).

the supplier and incubated for 1.5 h (room temperature). For the detection of IKB alpha, NF-κB p65 (p S536), and NF-κB p65 the NF-κB Signaling Pathway Antibody Sampler Panel (ab228529, Abcam) was used. L1 Cell Adhesion Molecule (L1CAM) was visualized with a mouse monoclonal antibody anti-L1CAM (ab 24345, Abcam). For the morphological characterization of the mitochondria the transport protein TOM20 was detected with anti-TOM20 (F-10) mouse monoclonal antibody (Sc-17764, Santa Cruz Biotechnology). After removal of the primary antibodies the Alexa Fluor 568 Donkey Anti-Rabbit (A10042_LOT2136776) and the Alexa Fluor 488 Donkey Anti-Mouse (A21202_LOT2090565) were used as secondary antibodies. After multiple washing steps, slides were mounted and sealed with Roti-Mount FluoCare (Roth, Graz, Austria) with DAPI. Images were acquired with a Confocal LSM Zeiss 710 equipped with an ELYRA PS.1 system. Structured illumination microscopy (SIM) images and confocal images were acquired with a Plan Apochromat 100×/1.46 oil objective or with a Plan Apochromat 63×/1.4 oil objective. Image analysis was performed with the software Zeiss ZEN.

Live Cell Imaging of Mitochondria and Membrane Morphology. For structural evaluation of the membrane THP-1 macrophages were stained with CellMask Deep Red Plasma Membrane Stain (1:1000 dilution, depicted in white). For superoxide quantification cells were stained with MitoTracker Green FM (1:1000 dilution, depicted in blue, indicated as MitoTracker) and MitoSOX Red mitochondrial superoxide indicator (1:1000 dilution, red to white, indicated as MitoSOX). Regions of interest (ROI) were identified using the MitoTracker as reference, and signal intensities were expressed as the MitoSox/MitoTracker ratio. Mitochondrial morphological features were evaluated offline with ImageJ software (Figure 3B) according to the method described by Valente and co-workers.[26] Staining solutions were diluted in Live Cell Imaging Solution (all from Molecular Probes, Life Technologies, Thermo Fisher Scientific, Waltham, USA). At the end of the staining, cells were rinsed and maintained in Live Cell Imaging Solution for the microscopy analysis. If not otherwise specified, optical fields ROI were quantified for every experimental setup from at least 4 independent cell preparations. Images were acquired with a Zeiss LSM 710 Confocal Microscope with the ELYRA PS.1 system for super-resolution with a Plan-Apochromat 63×/1.2 water objective and an Andor iXon 897 (EMCCD) camera.

Membrane Fluidity. Membrane fluidity was measured as previously described.[19] Briefly, cells were incubated for 1 h at 37 °C in a humidified incubator with 10 μM 1-pyrenedecanoic acid (PDA) diluted in Live Cell Imaging Solution. Afterward, cells were incubated with the respective stimuli, and fluorescence was immediately measured with a Cytation 3 Cell Imaging Multi-Mode Reader equipped with the Gen5 Data Analysis Software (BioTek Instruments, Inc., Winooski, Vermont, USA). The signal was calculated as the ratio between ex/em. 344/470 nm for the PDA excimers and ex/em. 344/375 for the monomeric form. *N*-Acetylcysteine (10 mM NAC, Figure 6A,B) was included as antioxidant (assay control). Data are mean of minimum 6 independent experiments performed in quadruplicates.

Lipid Peroxidation Assay. For the lipid peroxidation assay, ATXII (0.1 μM, 1 μM, and 10 μM), methyl-β-cyclodextrin (50 μM), ATXI

https://dx.doi.org/10.1021/acs.chemrestox.9b00378
Chem. Res. Toxicol. 2020, 33, 492−504

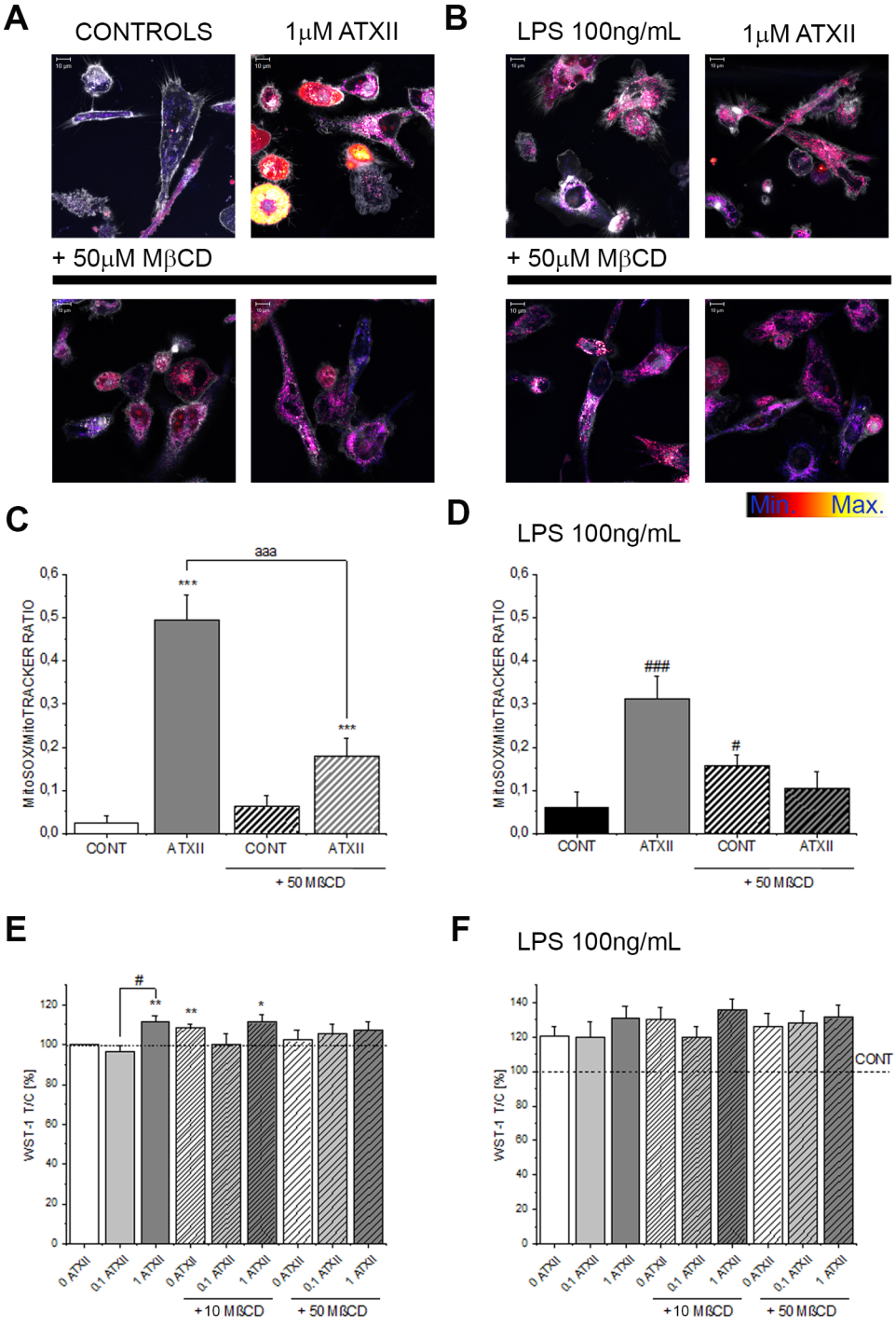

Figure 3. Effect of ATXII on the mitochondrial superoxide level in THP-1 macrophages. (A) Appearance of the mitochondria MitoSOX (red to white) and MitoTracker (blue) in control conditions or after incubation with 1 μM ATXII and/or 50 μM MβCD and in the presence of LPS 100 ng/mL (B). (C, D) MitoSOX/MitoTracker signal ratio. Image analysis was performed on $n \geq 90$ cells from 4 independent cell preparations. Symbols indicate difference *# $p < 0.05$ and ***### $p < 0.001$ in comparison to controls, aaa $p < 0.001$ comparison to ATXII Student's t-test. (E, F) WST-1 assay. Data are mean of $n = 6$ independent experiments. Symbols indicate difference * $p < 0.05$, ** $p < 0.01$ in comparison to controls, and # $p < 0.05$ in comparison to the ATXII 0.1 μM Mann−Whitney test. All concentrations are intended in [μM].

(1 μM), or H_2O_2 (1 mM, POS. CONT.) selected combinations and solvent control (0.1−0.4% DMSO) were applied to the macrophages in live cell imaging buffer (Thermo-Fisher Scientific). Treatments with compounds lasted for 1 h. After 1 h, a ratiometric lipid peroxidation sensor (Lipid peroxidation assay kit_ab 243377 Abcam) was added to the cells and incubated for 30 min. After 3 washing steps utilizing HHBS, images of cells were acquired within the next 2 h applying a confocal LSM Zeiss microscope equipped with ELYRA PS.1 and quantified as the FITC/TRITC signal ratio. Data are the result from the quantification of 45 ROI obtained from 3 independent cell preparations.

Statistical Analysis. Data were evaluated with the software OriginPro 2018b (OriginLab Corporation, Northampton, USA). Multiple comparison of independent samples was performed with the one-way ANOVA test followed by Fisher's test. Mann−Whitney (samples with $n < 10$) and Student's t-tests (samples with $n > 40$) were applied for the direct comparison of groups of data. Distributions were considered different using threshold values of 0.05.

https://dx.doi.org/10.1021/acs.chemrestox.9b00378
Chem. Res. Toxicol. 2020, 33, 492−504

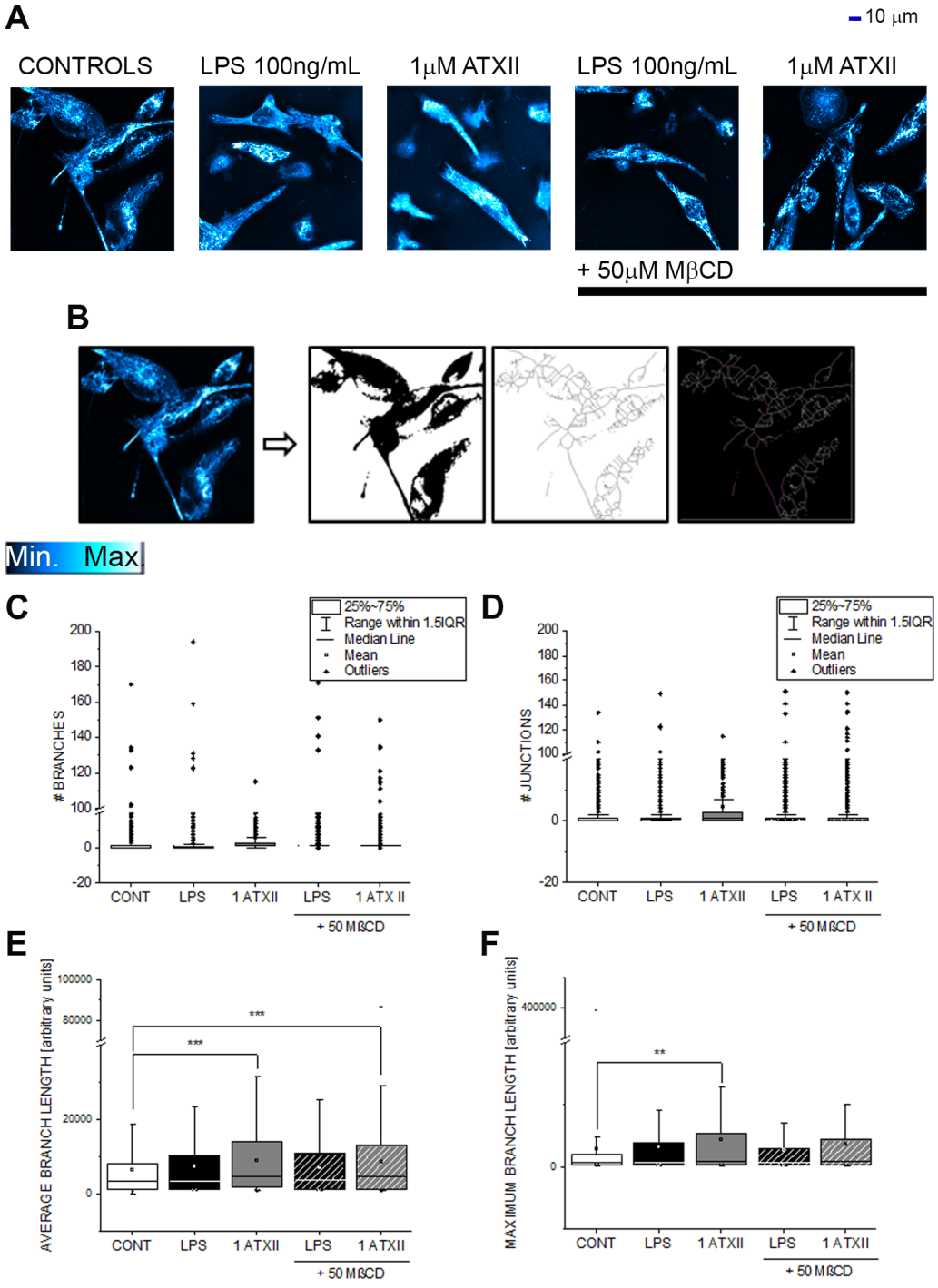

Figure 4. Effect of ATXII on mitochondrial morphology in THP-1 macrophages. (A) Appearance of mitochondria (1 h incubation LPS, 1 μM ATXII with or without 50 μM MβCD). (B) Image processing workflow. Number of branches (C), junctions (D), average (E), and maximum (F) branch length. Data are representative of total mitochondrial quantification from $n \geq 11$ optical fields acquired from 4 independent cell preparations. Symbols indicate difference ** $p < 0.01$, *** $p < 0.001$ Student's t-test. All concentrations are intended in [μM].

RESULTS

Effect of Altertoxin II on NF-κB Activation Pathway. In order to obtain the first insight into the potential of ATXII to modulate inflammatory cascades, we measured the effect of the mycotoxin on the activation of the transcription factor NF-κB (nuclear factor-κB). NF-κB is a crucial regulator of inflammatory cascades as for instance sustaining the activation of TNFα, Toll-like receptors (TLRs), and IL-1β.[27,28] In THP-1 monocytes, ATXII caused a concentration dependent decrease in the activation of the transcription factor (Figure 1A), without inducing toxicity (Figure 1B). Moreover, since ATXII is known to impair cell membrane functionality[19] and inflammatory cascades rely on membrane structural organization and distribution of the transmembrane receptors,[29,30] MβCD (10−50 μM) was also included in the experimental layout. MβCD can be used to deplete the cell membrane of cholesterol,[31] thus altering the cholesterol-rich domains (rafts) that host the TLRs.[30] Intriguingly, when ATXII was coincubated with MβCD, the NF-κB luciferase activity could be detected again at levels comparable to those of

https://dx.doi.org/10.1021/acs.chemrestox.9b00378
Chem. Res. Toxicol. 2020, 33, 492−504

controls (Figure 1A). In addition, considering the capability of another toxin produced by *Alternaria* fungi, namely alternariol to suppress the effect of bacterial lipopolysaccharide (LPS),[12,32] we also verified the potential crosstalk between ATXII and LPS (Figure 1C). Even though a tendency toward the decrease in the signal was observed, no significant effect was detectable under these experimental conditions. Measurement of the cell viability with WST-1 assay revealed for cells incubated with ATXII and LPS a very prominent increase in reagent absorbance, compatible with an enhanced capability of the monocytes to metabolize the tetrazolium salts into formazan.[33]

In order to confirm also in differentiated THP-1 macrophages the relevance of the data observed in the monocytes, immunofluorescence experiments were performed using as reference key proteins of the NF-κB pathway, namely IKB alpha, NF-κB p65 (p S536), and NF-κB p65. Immunolocalization of IKB alpha revealed no major differences between stimulated cells (ATXII or LPS) and controls (Figure 2A). However, the NF-κB p65 subunit presented clear nuclear localization after incubation with LPS (1 h, LPS 100 ng/mL), which was not observable for the mycotoxin (Figure 2B and D). The phosphorylated subunit NF-κB p65 (p S536), which is associated with p65 turnover,[34] showed a tendency toward an increase in ATXII-incubated macrophages (Figure 2C, D) in comparison to controls, thus supporting overall a coherent interpretation with the data of the reporter gene assay.

Effect of Altertoxin II on Mitochondrial Function and Morphology. Once having ascertained the potential of ATXII to modulate NF-κB activation, we started to investigate the mechanisms potentially sustaining this effect on THP-1 macrophages. ATXII was previously described to induce oxidative stress,[18,19] and reactive oxygen species (ROS) can modulate the activation of NF-κB signaling at multiple levels,[20,35] including being responsible for the suppression of the activation of the transcription factor.[36] Accordingly, we investigated the effects of the mycotoxin alone or in combination with LPS and MβCD at the mitochondrial level. Evaluation of the mitochondrial superoxide ion (as MitoSox/MitoTracker ratio) revealed a significant increase triggered by 1 μM ATXII (Figure 3A–D; 1 h incubation). This response was reduced by the coincubation with 50 μM MβCD and/or LPS (100 ng/mL; Figure 3A–D). In addition, WST-1 assay performed on macrophages confirmed the capability of ATXII to increase the metabolism of the tetrazolium salts, and as for the mitochondrial superoxide, this effect was also modulated by the presence of MβCD (Figure 3E). The coincubation with LPS increased significantly the WST-1 signals in all the experimental conditions (Figure 3F).

Since we could ascribe an effect of ATXII on mitochondria of THP-1 macrophages, both directly through the evaluation of the superoxide ion and indirectly through the metabolism of WST-1 dye, we performed also detailed morphological analysis of the mitochondrial structure. Mitochondrial morphology is tightly related to the metabolic activity[37] and plays consequently a prominent role in determining the energetic balance necessary for the immune cells.[23] The number of branches and the number of junctions in the mitochondria network remained constant in all the experimental conditions (Figure 4A, C, and D). Incubation with ATXII resulted in a prominent morphological alteration of the mitochondria that resulted in an increase in the detected average and the maximum length of the mitochondrial branches (Figure 4E, F), and these responses were partially diminished by the incubation with MβCD (Figure 4F). However, in order to further clarify if these results could be attributed to changes in morphology and/or distribution of the organelles, immunofluorescence experiments followed by Structured Illumination Microscopy (SIM) were also performed (Figure 5A). Indeed,

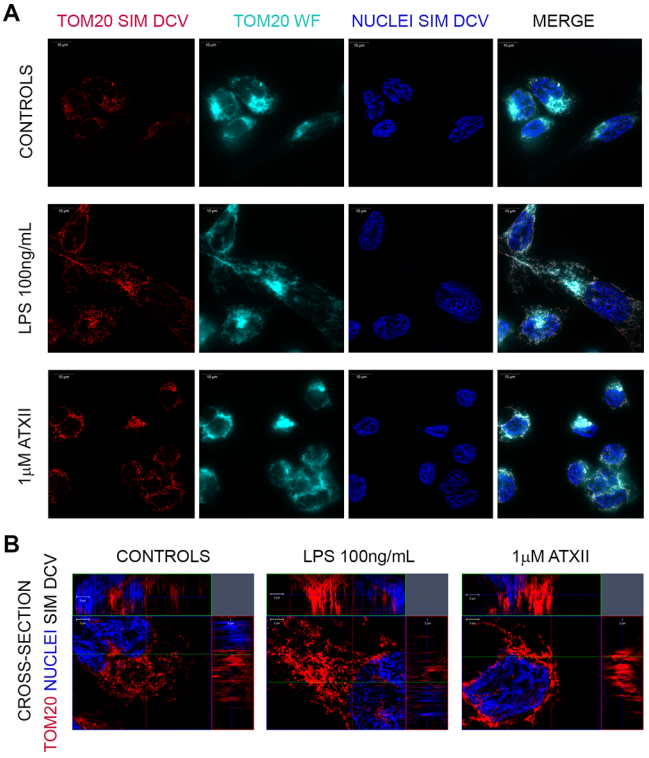

Figure 5. Representative images of the immunolocalization of the mitochondrial protein TOM20 in THP-1 macrophages. (A) Appearance of TOM20 after application of structured illumination microscopy SIM with deconvolution rendering (DCV, red) or wide field rendering (WF, light blue). Nuclei depicted in blue (DCV rendering). (B) Details of the cross-section of the 3D SIM DCV images. Scale bars 10 μm for panel A and 2 μm for panel B.

upon activation with LPS the mitochondria network expanded toward the periphery of the cells, whereas incubation with the mycotoxin induced the formation of a tightly packed network localized in the perinuclear region (Figure 5B).

Effect of Altertoxin II on Membrane Structure and Biophysical Properties. Since ATXII caused a significant increase in the mitochondrial superoxide level, we investigated the effects of the toxin on membrane fluidity. In fact, it was previously demonstrated that membrane rigidification, as for instance in relation to oxidative insult, could impair the response capability of macrophages.[38,39] In our experimental conditions, MβCD induced a concentration dependent decrease in membrane fluidity in THP-1 macrophages; however, we could not observe any significant effect attributable to the toxin. Of note, the use of the antioxidant NAC was possible only in the limited time frame of the incubation necessary for the membrane fluidity assay (max. 10 min) since the significant increase in the membrane fluidity (Figure 6A, B) was accompanied shortly after by a loss of cell adherence.

Since the PDA membrane fluidity assay was limited in our experimental conditions to very short incubation times, we evaluated the effect of the toxin alone or in combination with MβCD and LPS on the membrane morphology (Figure 6C, D). Indeed, incubation with ATXII was associated with an increased intensity of the fluorescence signal of the membrane (Figure 6E), and this effect was reduced by the coincubation with MβCD.

https://dx.doi.org/10.1021/acs.chemrestox.9b00378
Chem. Res. Toxicol. 2020, 33, 492–504

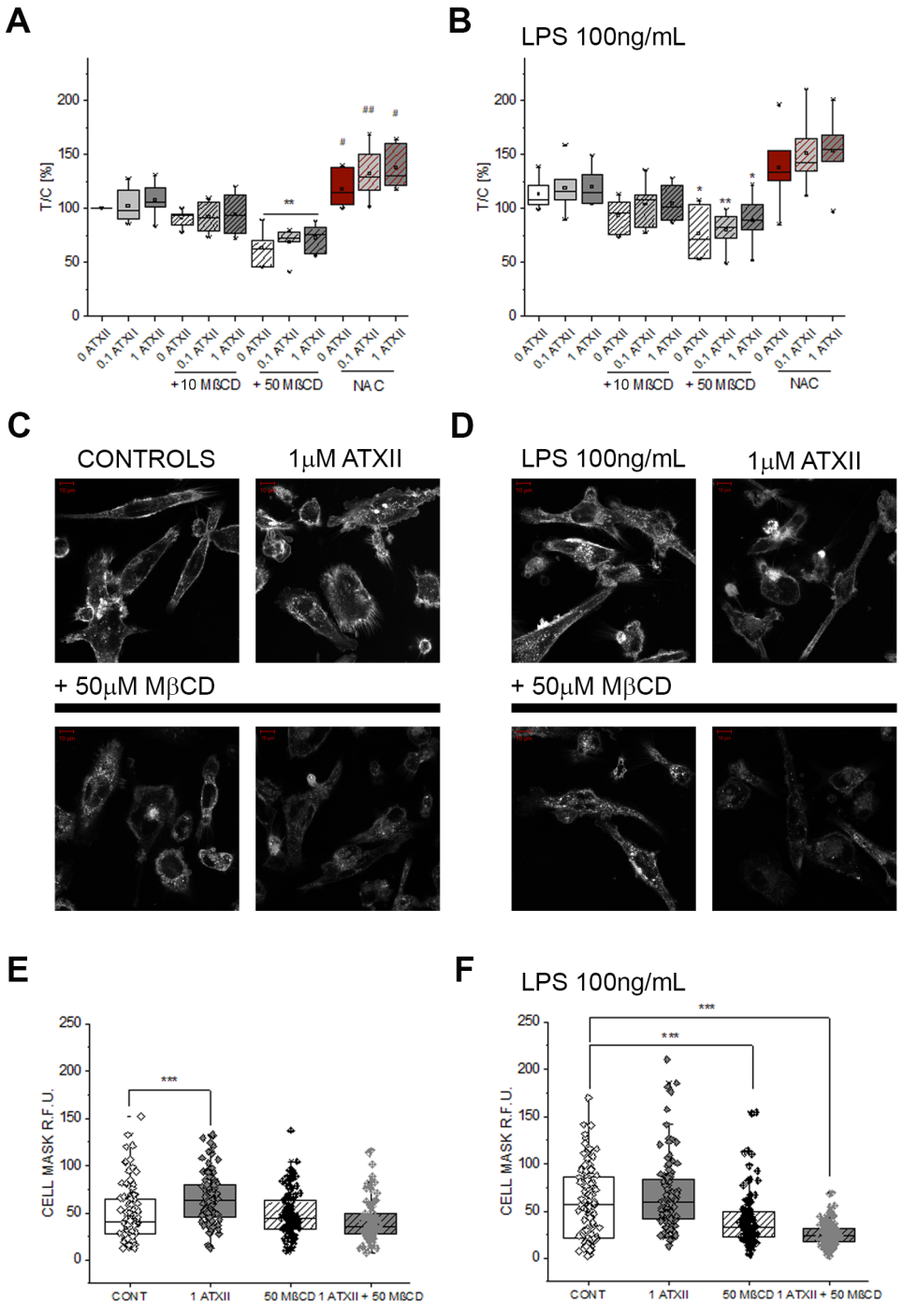

Figure 6. Effect of ATXII on the membrane of THP-1 macrophages. (A, B) Membrane fluidity assay. Data are mean of $n \geq 6$ independent experiments performed in quadruplicate. Symbols *# ($p < 0.05$) and ** ## ($p < 0.01$) indicate significant decrease (*) or increase (#) in comparison to controls Mann−Whitney test. (C, D) Morphological characterization of the cell membrane in control conditions or after incubation with 1 μM ATXII and/or 50 μM MβCD and in the presence of LPS 100 ng/mL. (E, F) CellMask signal quantification (RFU). Image analysis was performed on $n \geq 90$ cells from 4 independent cell preparations. Symbols indicate difference *** $p < 0.001$ Student's t-test. All concentrations are intended in [μM].

Similarly, the membrane signal measured in the presence of LPS was modulated by the coincubation with MβCD and ATXII (Figure 6F).

Moreover, since the toxin appeared able to modify the structure of the membrane, we further investigated if this event could be accompanied by an altered localization of transmembrane proteins. In particular, we focused on L1CAM which is known to modulate the inflammatory cascade via a crosstalk with NF-κB.[40,41] Indeed, immunolocalization of L1CAM showed that both LPS and ATXII stimulations were able to increase the signal of the protein (Figure 7A, B). However, the signal elicited by the mycotoxin appeared more concentrated and localized in defined areas, whereas the one of LPS seemed more evenly diffused within the cells (Figure 7A, C).

Effect of Altertoxin II on Lipid Peroxidation and Structure−Activity Relationship. In light of the capability of ATXII to alter the membrane structure fluorescence localization, we decided to investigate in more detail if the toxin could

https://dx.doi.org/10.1021/acs.chemrestox.9b00378
Chem. Res. Toxicol. 2020, 33, 492−504

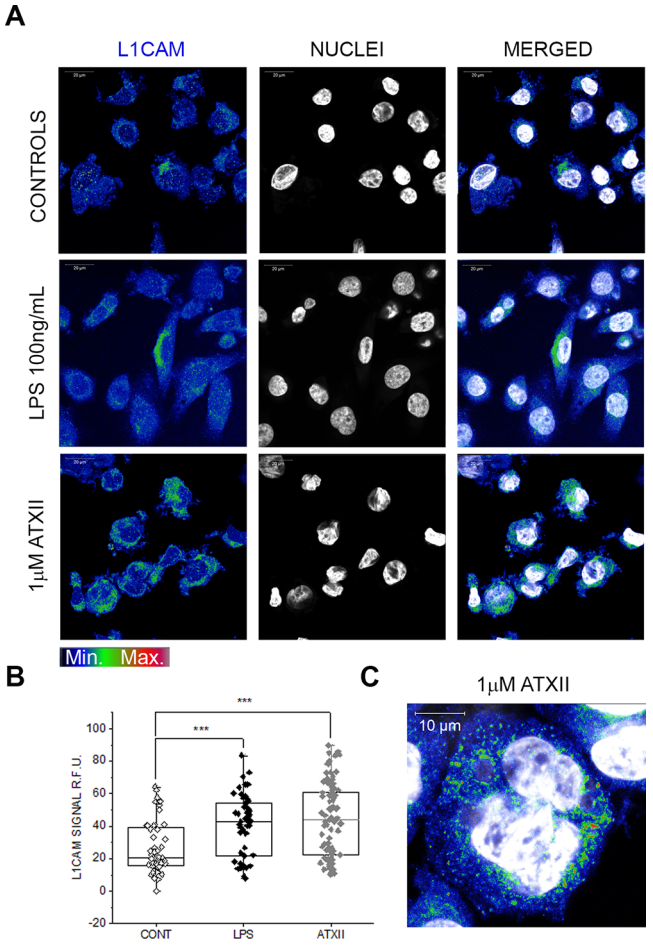

Figure 7. Representative images of the immunolocalization of L1CAM in THP-1 macrophages. (A) Appearance of L1CAM in controls or after incubation with 1 μM ATXII or LPS 100 ng/mL. (B) Fluorescence signal analysis after immunodetection of L1CAM data are mean ± SE of $n > 50$ ROI from 3 independent cell preparations. Symbols indicate difference *** $p < 0.001$ at Student's t-test. (C) Details of the immunolocalization of L1CAM after incubation with ATXII.

trigger lipid peroxidation in THP-1 macrophages. After 1 h incubation, we were able to detect a concentration dependent increase in the signal generated in the lipid peroxidation assay (Figures 8A, C). Incubation with ATXII triggered a signal increase comparable to the one of the positive control (H_2O_2 1 mM, Figure 8A, C), and this effect remained stable regardless of the coincubation with MβCD (Figure 8C). Moreover, in light of the structural similarity, the mycotoxin ATXI was used as control to evaluate the contribution of the epoxide moiety in the potential of ATXII to induce lipid or mitochondrial alterations in THP-1 macrophages (Figure 8B, D). The lack of the epoxide group was indeed accompanied by a respective loss of the lipid-peroxidation activity (Figure 8B, C) and decreased potential to induce mitochondrial superoxide or changes in membrane morphology (Figure 8E, F).

Effect of Cholesterol Supplementation on the Mechanism of Action of Altertoxin II. Since our data pointed toward a crucial role for membrane structure and cholesterol in mediating the effects of ATXII on THP-1 macrophages, proof of principle experiments were performed also in the presence of water-soluble cholesterol (cholesterol−methyl-β-cyclodextrin). Loading the cells with 10 μM cholesterol-MβCD induced an increase in the mitochondrial superoxide, as well as the formation of dense areas on the cell membrane (Figure 9A, B). Coincubation with ATXII exacerbated the effect of the mycotoxin leading to a more pronounced increase in the mitochondrial superoxide signal and a faster loss of morphology of THP-1 macrophages (Figure 9A, C), thus contributing to delineation of the role of cholesterol in sustaining the effect of the toxin.

DISCUSSION

With the discovery and deeper characterization of the immunomodulatory potential of *Alternaria alternata* fungi,[4,9,10,32,42,43] there is a rising need for the comprehension of the immunotoxicological potential of the secondary metabolites produced by these molds. This includes the commercially available compounds, such as alternariol,[4,11,12,42,44] as well as other mycotoxins that can be produced by *Alternaria alternata*. The perylene quinone altertoxin II (ATXII) is a well characterized genotoxic compound;[13,14] however, its impact with respect to immuno modulatory potential was never investigated so far. Taking this as a starting point, we screened the potential of ATXII to regulate one of the most important transcription factors governing inflammation, namely NF-κB.[27,28,45,46] NF-κB is also often used as a benchmark in describing the immunomodulatory potential of compounds of natural origin as, for instance, food constituents[47−50] or mycotoxins.[12,51,52] Intriguingly, ATXII reduced NF-κB activation in a subtoxic concentration range (Figure 1), and unlike LPS, it did not trigger the nuclear translocation of NF-κB subunit p65 (Figure 2). The ATXII mechanism of action appeared dependent on the plasma membrane structure, since it was abolished by cholesterol depletion using MβCD (Figure 1). Moreover, the above-mentioned findings were opposite to what could be expected from an alteration of the membrane integrity and/or increased toxin permeability. Indeed, crosstalk between plasma membrane and inflammation is much more complex. For example, the transmembrane protein L1CAM is necessary for constitutive regulation of NF-κB,[40] and it was recently demonstrated that L1CAM can be also shuttled from the plasma membrane to the mitochondria,[53] thus sustaining a direct connection between membrane structural proteins, mitochondria, and inflammation. In line, in our experimental setup, ATXII altered not only membrane morphology (Figure 6) but also the immunolocalization of L1CAM (Figure 7) and mitochondrial appearance (Figures 4 and 5). Mitochondria play a central role in sustaining the efficiency and the activation of the immune system.[23] Very specific fingerprinting in the ROS production is strictly related to the activation status of immune cells,[21] and ROS signaling can impact NF-κB upstream and downstream.[20,36,54] For example, binding of the transcription factor is directly related to the cellular glutathione homeostasis, and a loss of the binding capacity was related to an increase in the oxidized form GSSG.[55] Similarly, oxidized low-density lipoproteins were described to suppress DNA-binding activity of NF-κB,[56] and the Nrf2 binding protein KEAP-1 was also described to bind IKKβ leading to suppression of NF-κB activity.[57] The perylene quinone mycotoxin ATXII is known to induce oxidative stress and, at least in short-term incubation, to deplete reduced glutathione pools *in vitro*.[18,19] Moreover, ATXII can also trigger the release of Nrf2 from its binding protein KEAP-1 with the subsequent nuclear translocation of the transcription factor,[18,19] thus potentially increasing the availability of "free" KEAP-1 that could contribute in sustaining the immunosuppressive effect of the mycotoxin. Considering the multiple possibilities for crosstalk between oxidative stress and inflammation/immunomodulation, we started to investigate the effect of the toxin on mitochondrial

https://dx.doi.org/10.1021/acs.chemrestox.9b00378
Chem. Res. Toxicol. 2020, 33, 492−504

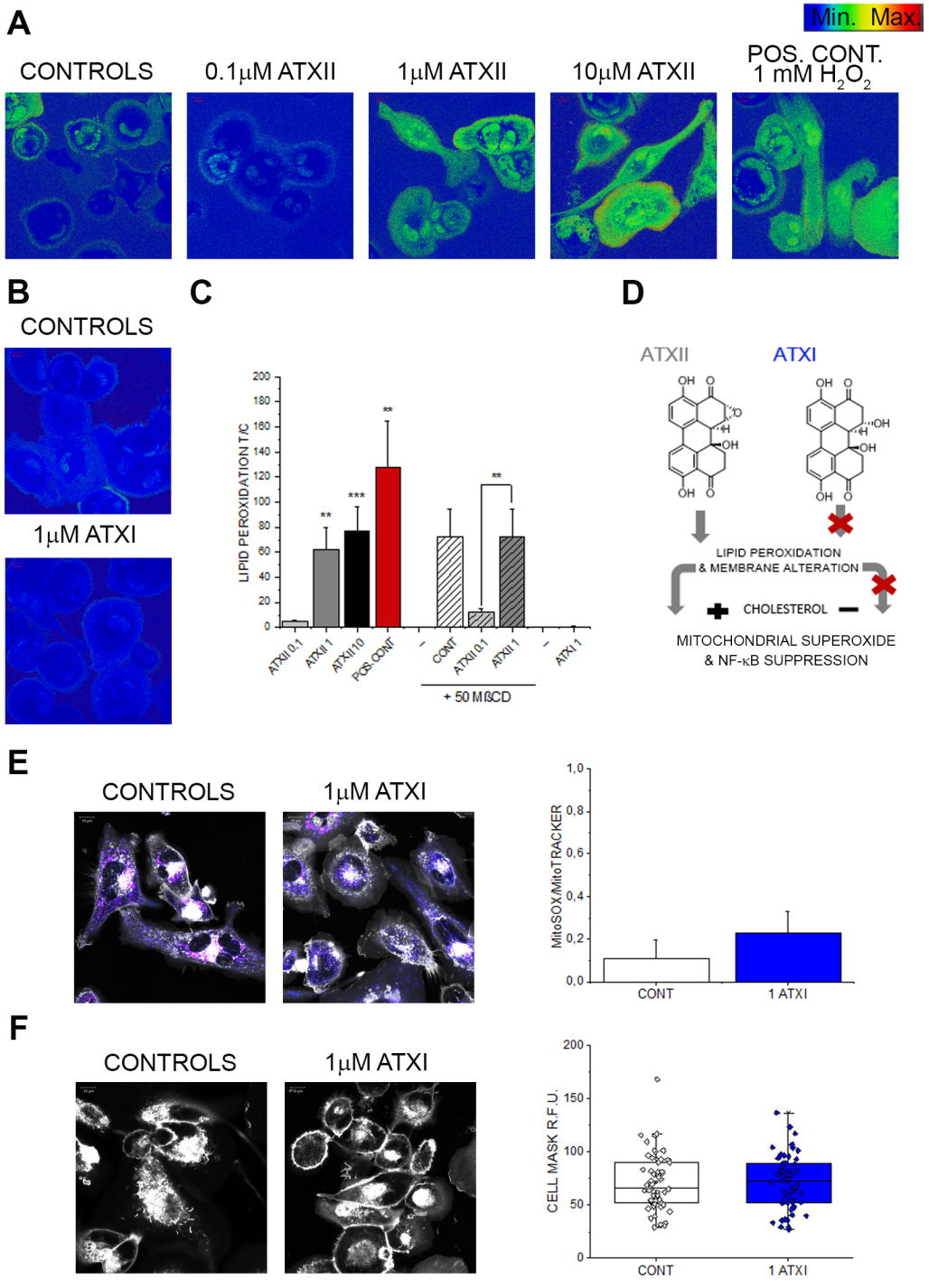

Figure 8. Effect of ATXII on the lipid peroxidation in THP-1 cells. (A, B) Appearance of THP-1 macrophages FITC/TRITC signal ratio lipid peroxidation quantification. (C) Quantification of the lipid peroxidation signal. (D) Data summary in relation to structural differences between ATXII and ATXI. Effect of ATXI on the mitochondrial superoxide production (E) and membrane (F). Data are mean ± SE of $n \geq 45$ ROI obtained from 3 independent cell preparations, and direct comparison was performed with Student's *t*-test ** $p < 0.01$ and *** $p < 0.001$. Positive controls (POS. CONT) 1 mM H_2O_2, all other concentrations are intended in [μM]. Scale bars for the figures 10 μm.

superoxide production in macrophages. Interestingly, we observed within 1 h of incubation with the toxin a significant increase in the mitochondrial superoxide, which could mirror both the pro-oxidative potential of the toxin,[18,19] as well as the activation of immune cells[21] (Figure 3). However, as described also for the NF-κB activation, the response triggered by the mycotoxin differed substantially from that of LPS. The effect of ATXII was accompanied by an alteration of the mitochondrial morphology with an increase in the average/maximum length of the mitochondrial branches. However, the above-mentioned result was possibly related to the high density of the mitochondrial signal observable in the pictures, and it was also compatible with a reorganization of the organelles or intracellular recruitment rather than exclusively to an increase in the fused mitochondria (Figure 4). Super-resolution structured illumination microscopy allowed to observe in 3D the distribution of the mitochondria upon activation and revealed for the cells incubated with the mycotoxin the formation of dense areas of accumulation in

https://dx.doi.org/10.1021/acs.chemrestox.9b00378
Chem. Res. Toxicol. 2020, 33, 492−504

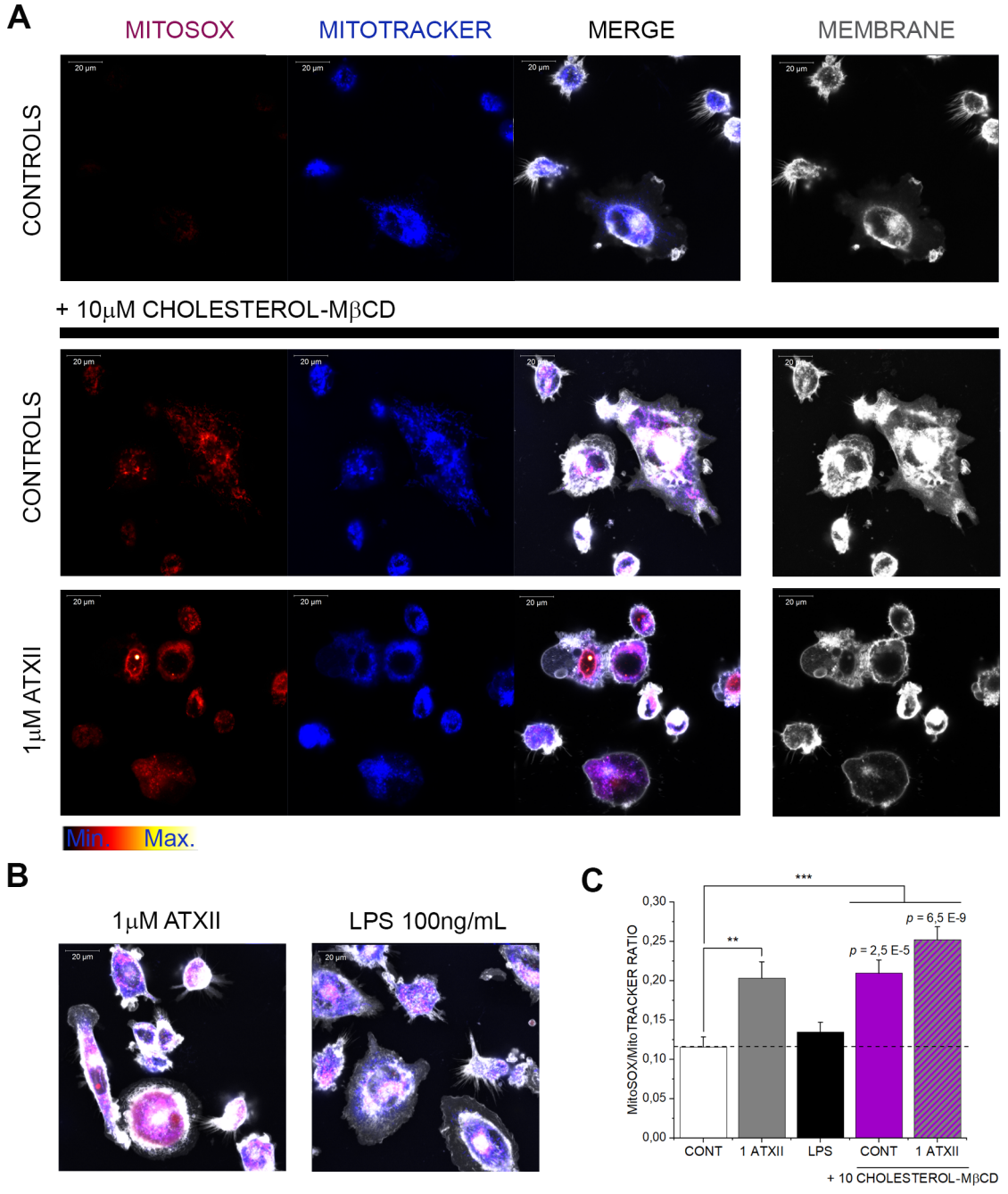

Figure 9. Role of cholesterol load in the capability of ATXII to induce mitochondrial superoxide. (A) The MitoSOX signal is indicated by a red (Min.) to white (Max.) signal, MitoTracker for the localization of the mitochondria is indicated in blue, and plasma membrane is depicted in white (CellMask). (B) Appearance of THP-1 macrophages incubated with ATXII and LPS. (C) Quantification of the MitoSOX/MitoTracker signal ratio. Data are mean ± SE of $n > 55$ cells obtained from 3 independent cell preparations. Symbols indicate difference ** $p < 0.01$ and *** $p < 0.001$ Student's *t*-test.

the perinuclear region (Figure 5) and for the LPS-stimulated cells the organization of a more distributed network. Of note, superoxide production is generally associated with a high NADH/NAD+ ratio,[58] and this effect could contribute to the enhanced WST-1 metabolism that was detected at several levels in the presence of ATXII (Figure 1B, C and Figure 3E, F). Both functional (superoxide production, Figure 3) and partially structural (morphological changes and reorganization, Figure 4) effects of ATXII at the mitochondrial level were modulated by the presence of MβCD. This could imply that molecular events could occur also upstream to this point and connect THP-1 macrophages cholesterol content/membrane structure to the effects on mitochondrial superoxide production and NF-κB transcription. We previously demonstrated that the toxicological potential of ATXII on intestinal cells is sustained by profound alteration of membrane biophysical properties, albeit in a cell type-dependent manner.[19] Hence, the question arose if similar mechanisms could be of relevance for THP-1 macrophages. Membrane biophysical properties, namely membrane fluidity, play a central role in sustaining the proinflammatory cascade in THP-1 macrophages.[38] In addition, pro-oxidative insults (H_2O_2) and respective increase in lipid peroxidation were described to induce formation of rigid areas on the cell surface and to decrease membrane fluidity, ultimately modulating inflammatory outcome.[39]

https://dx.doi.org/10.1021/acs.chemrestox.9b00378
Chem. Res. Toxicol. 2020, 33, 492−504

In our experimental conditions, incubation with ATXII was not accompanied by an alteration of membrane fluidity; however, the PDA assay primarily reflects short-term response (10 min incubation). When evaluating the cell membrane morphology (after 1 h incubation), we measured a significant increase in the signal associated with the CellMask staining dye in cells incubated with 1 μM ATXII (Figure 6C, E). This effect was possibly attributable to an altered turnover/intercalation of the fluorescent marker and was abolished by coincubation with MβCD (Figure 6C, E). In line, we decided to verify the potential of ATXII to impact directly lipid peroxidation and observed a concentration-dependent effect of the mycotoxin (Figure 8A, C). Intriguingly, the cholesterol complexing agent MβCD triggered lipid peroxidation *per se* (Figure 8C), and it is possible that this event could contribute, together with cholesterol depletion, to the reduction of membrane fluidity measured in THP-1 cells (Figure 6). Coincubation of MβCD with ATXII did not alter the response profile of the mycotoxin, thus implying, on the one hand, that the effect of the toxin on lipid peroxidation is independent from the presence of cholesterol and, on the other hand, that cholesterol is probably crucial in modulating the effect of the toxin downstream from this point. In line, we observed that the capability of ATXII to induce superoxide ion increase in the mitochondria was reduced by cholesterol depletion with MβCD (Figure 3), and the effect on the rearrangement of mitochondria morphology was also modulated (Figure 4). In addition, experiments performed with increased load of cholesterol (cholesterol-MβCD) enhanced the toxicity of ATXII and the potential of the mycotoxin to induce mitochondrial superoxide (Figure 9). Intriguingly, it was recently described that cholesterol trafficking and homeostasis is crucial for inflammasome activation.[59] Moreover, cholesterol appears to be essential for the retrograde transport of the mitochondria at the nuclear level as a consequence of ROS stress; anchoring of the organelles on the nuclear surface seems to occur thanks to the formation of mitonuclear contact sites rich in oxysterols obtained after oxidation of cholesterol.[60] Mitochondrial retrograde transport in the nuclear region was previously described to support cell necessity to increase transcription of detoxification enzymes after ROS insult,[61] and mitochondrial perinuclear accumulation upon incubation with ATXII (Figure 5) strongly suggests a similar mechanism. In line, we previously demonstrated that ATXII can increase the gene transcription of gamma-glutamate cysteine ligase in HT-29 cells in relation to increased oxidative stress and Nrf2 translocation.[18] Experiments performed with ATXI suggest the lipid peroxidation to be directly related to the pro-oxidative capacity of the molecule, since the scaffold of the toxin deprived from the epoxide moiety failed to mediate the membrane morphological alterations and the lipid peroxidation triggered by ATXII (Figure 8B–D, F).

In conclusion, we described the effect of ATXII on THP-1 macrophages *in vitro*. The mycotoxin induced lipid peroxidation thanks to the presence of the epoxide group and this effect down-streamed at the intracellular level in the presence of membrane cholesterol inducing mitochondrial superoxide production, mitochondria reorganization, and suppression of the transcription factor NF-κB. These molecular events describe a novel effect of ATXII that is exerted in concentrations typically subtoxic. Overall, our results open new perspectives in the interpretation of the immune-modulatory potential of fungi *Alternaria alternata* that can proliferate also in the domestic environment.

AUTHOR INFORMATION

Corresponding Author

Giorgia Del Favero − *Department of Food Chemistry and Toxicology, Faculty of Chemistry and Core Facility Multimodal Imaging, Faculty of Chemistry, University of Vienna, 1090 Vienna, Austria;* orcid.org/0000-0001-8633-5458; Email: giorgia.del.favero@univie.ac.at

Authors

Julia Hohenbichler − *Department of Food Chemistry and Toxicology, Faculty of Chemistry, University of Vienna, 1090 Vienna, Austria*

Raphaela Maria Mayer − *Department of Food Chemistry and Toxicology, Faculty of Chemistry, University of Vienna, 1090 Vienna, Austria*

Michael Rychlik − *Chair of Analytical Food Chemistry, Technical University of Munich, 85354 Freising, Germany*

Doris Marko − *Department of Food Chemistry and Toxicology, Faculty of Chemistry, University of Vienna, 1090 Vienna, Austria;* orcid.org/0000-0001-6568-2944

Complete contact information is available at: https://pubs.acs.org/10.1021/acs.chemrestox.9b00378

Author Contributions

G.D.F. planned the research and together with J.H. and R.M.M. performed the experiments and data analysis. D.M. and M.R. contributed materials and reagents. The manuscript was written thanks to the contributions of all authors. All authors have given approval to the final version of the manuscript.

Funding

This work was supported by the University of Vienna.

Notes

The authors declare no competing financial interest.

ACKNOWLEDGMENTS

The authors are grateful to Endre Kiss, Eva Attakpah, and Michael Zeugswetter for skillful technical help and Christopher Gerner for stimulating and supportive discussions. The authors acknowledge the support of the Core Facility Multimodal Imaging of the Faculty of Chemistry member of VLSI (Vienna Life Science Instruments).

REFERENCES

(1) Gu, M. J., Han, S. E., Hwang, K., Mayer, E., Reisinger, N., Schatzmayr, D., Park, B. C., Han, S. H., and Yun, C. H. (2019) Hydrolyzed fumonisin B1 induces less inflammatory responses than fumonisin B1 in the co-culture model of porcine intestinal epithelial and immune cells. *Toxicol. Lett. 305*, 110−116.

(2) Li, Y., Fan, Y., Xia, B., Xiao, Q., Wang, Q., Sun, W., Zhang, H., and He, C. (2017) The immunosuppressive characteristics of FB1 by inhibition of maturation and function of BMDCs. *Int. Immunopharmacol. 47*, 206−211.

(3) Pierron, A., Bracarense, A., Cossalter, A. M., Laffitte, J., Schwartz-Zimmermann, H. E., Schatzmayr, G., Pinton, P., Moll, W. D., and Oswald, I. P. (2018) Deepoxy-deoxynivalenol retains some immune-modulatory properties of the parent molecule deoxynivalenol in piglets. *Arch. Toxicol. 92* (11), 3381−3389.

(4) Solhaug, A., Karlsøen, L. M., Holme, J. A., Kristoffersen, A. B., and Eriksen, G. S. (2016) Immunomodulatory effects of individual and combined mycotoxins in the THP-1 cell line. *Toxicol. In Vitro 36* (Supplement C), 120−132.

(5) Pestka, J. J. (2010) Deoxynivalenol: mechanisms of action, human exposure, and toxicological relevance. *Arch. Toxicol. 84* (9), 663−79.

(6) Liao, Y., Peng, Z., Chen, L., Nussler, A. K., Liu, L., and Yang, W. (2018) Deoxynivalenol, gut microbiota and immunotoxicity: A potential approach? *Food Chem. Toxicol. 112*, 342−354.
(7) Atan Sahin, O., Kececioglu, N., Serdar, M., and Ozpinar, A. (2016) The association of residential mold exposure and adenotonsillar hypertrophy in children living in damp environments. *International journal of pediatric otorhinolaryngology 88*, 233−8.
(8) Castanhinha, S., Sherburn, R., Walker, S., Gupta, A., Bossley, C. J., Buckley, J., Ullmann, N., Grychtol, R., Campbell, G., Maglione, M., Koo, S., Fleming, L., Gregory, L., Snelgrove, R. J., Bush, A., Lloyd, C. M., and Saglani, S. (2015) Pediatric severe asthma with fungal sensitization is mediated by steroid-resistant IL-33. *J. Allergy Clin. Immunol. 136* (2), 312−322.e7.
(9) Gabriel, M. F., Postigo, I., Tomaz, C. T., and Martinez, J. (2016) Alternaria alternata allergens: Markers of exposure, phylogeny and risk of fungi-induced respiratory allergy. *Environ. Int. 89*−*90*, 71−80.
(10) Gabriel, M. F., Postigo, I., Gutierrez-Rodriguez, A., Sunen, E., Guisantes, J. A., Fernandez, J., Tomaz, C. T., and Martinez, J. (2016) Alt a 15 is a new cross-reactive minor allergen of Alternaria alternata. *Immunobiology 221* (2), 153−60.
(11) Solhaug, A., Holme, J. A., Haglund, K., Dendele, B., Sergent, O., Pestka, J., Lagadic-Gossmann, D., and Eriksen, G. S. (2013) Alternariol induces abnormal nuclear morphology and cell cycle arrest in murine RAW 264.7 macrophages. *Toxicol. Lett. 219* (1), 8−17.
(12) Kollarova, J., Cenk, E., Schmutz, C., and Marko, D. (2018) The mycotoxin alternariol suppresses lipopolysaccharide-induced inflammation in THP-1 derived macrophages targeting the NF-kappaB signalling pathway. *Arch. Toxicol. 92* (11), 3347−3358.
(13) Schwarz, C., Tiessen, C., Kreutzer, M., Stark, T., Hofmann, T., and Marko, D. (2012) Characterization of a genotoxic impact compound in Alternaria alternata infested rice as Altertoxin II. *Arch. Toxicol. 86* (12), 1911−25.
(14) Fleck, S. C., Burkhardt, B., Pfeiffer, E., and Metzler, M. (2012) Alternaria toxins: Altertoxin II is a much stronger mutagen and DNA strand breaking mycotoxin than alternariol and its methyl ether in cultured mammalian cells. *Toxicol. Lett. 214* (1), 27−32.
(15) Puntscher, H., Hankele, S., Tillmann, K., Attakpah, E., Braun, D., Kutt, M. L., Del Favero, G., Aichinger, G., Pahlke, G., Hoger, H., Marko, D., and Warth, B. (2019) First insights into Alternaria multi-toxin in vivo metabolism. *Toxicol. Lett. 301*, 168−178.
(16) Fleck, S. C., Sauter, F., Pfeiffer, E., Metzler, M., Hartwig, A., and Koberle, B. (2016) DNA damage and repair kinetics of the Alternaria mycotoxins alternariol, altertoxin II and stemphyltoxin III in cultured cells. *Mutat. Res., Genet. Toxicol. Environ. Mutagen. 798*−*799*, 27−34.
(17) Aichinger, G., Puntscher, H., Beisl, J., Kutt, M. L., Warth, B., and Marko, D. (2018) Delphinidin protects colon carcinoma cells against the genotoxic effects of the mycotoxin altertoxin II. *Toxicol. Lett. 284*, 136−142.
(18) Jarolim, K., Del Favero, G., Pahlke, G., Dostal, V., Zimmermann, K., Heiss, E., Ellmer, D., Stark, T. D., Hofmann, T., and Marko, D. (2017) Activation of the Nrf2-ARE pathway by the Alternaria alternata mycotoxins altertoxin I and II. *Arch. Toxicol. 91* (1), 203−216.
(19) Del Favero, G., Zaharescu, R., and Marko, D. (2018) Functional impairment triggered by altertoxin II (ATXII) in intestinal cells in vitro: cross-talk between cytotoxicity and mechanotransduction. *Arch. Toxicol. 92*, 3535−3547.
(20) Morgan, M. J., and Liu, Z.-g. (2011) Crosstalk of reactive oxygen species and NF-κB signaling. *Cell Res. 21* (1), 103−115.
(21) Gerner, M. C., Niederstaetter, L., Ziegler, L., Bileck, A., Slany, A., Janker, L., Schmidt, R. L. J., Gerner, C., Del Favero, G., and Schmetterer, K. G. (2019) Proteome Analysis Reveals Distinct Mitochondrial Functions Linked to Interferon Response Patterns in Activated CD4+ and CD8+ T Cells. *Front. Pharmacol. 10*, 727.
(22) Simula, L., Campanella, M., and Campello, S. (2019) Targeting Drp1 and mitochondrial fission for therapeutic immune modulation. *Pharmacol. Res. 146*, 104317.
(23) Mills, E. L., Kelly, B., and O'Neill, L. A. J. (2017) Mitochondria are the powerhouses of immunity. *Nat. Immunol. 18*, 488.
(24) Liu, Y., and Rychlik, M. (2015) Biosynthesis of seven carbon-13 labeled Alternaria toxins including altertoxins, alternariol, and alternariol methyl ether, and their application to a multiple stable isotope dilution assay. *Anal. Bioanal. Chem. 407* (5), 1357−69.
(25) Del Favero, G., Woelflingseder, L., Braun, D., Puntscher, H., Kutt, M. L., Dellafiora, L., Warth, B., Pahlke, G., Dall'Asta, C., Adam, G., and Marko, D. (2018) Response of intestinal HT-29 cells to the trichothecene mycotoxin deoxynivalenol and its sulfated conjugates. *Toxicol. Lett. 295*, 424−437.
(26) Valente, A. J., Maddalena, L. A., Robb, E. L., Moradi, F., and Stuart, J. A. (2017) A simple ImageJ macro tool for analyzing mitochondrial network morphology in mammalian cell culture. *Acta Histochem. 119* (3), 315−326.
(27) Zhang, Y. H., Lin, J. X., and Vilcek, J. (1990) Interleukin-6 induction by tumor necrosis factor and interleukin-1 in human fibroblasts involves activation of a nuclear factor binding to a kappa B-like sequence. *Mol. Cell. Biol. 10* (7), 3818−23.
(28) Hayden, M. S., and Ghosh, S. (2004) Signaling to NF-kappaB. *Genes Dev. 18* (18), 2195−224.
(29) Köberlin, M. S., Heinz, L. X., and Superti-Furga, G. (2016) Functional crosstalk between membrane lipids and TLR biology. *Curr. Opin. Cell Biol. 39* (Supplement C), 28−36.
(30) Plociennikowska, A., Hromada-Judycka, A., Borzecka, K., and Kwiatkowska, K. (2015) Co-operation of TLR4 and raft proteins in LPS-induced pro-inflammatory signaling. *Cell. Mol. Life Sci. 72* (3), 557−81.
(31) Lopez, C. A., de Vries, A. H., and Marrink, S. J. (2013) Computational microscopy of cyclodextrin mediated cholesterol extraction from lipid model membranes. *Sci. Rep. 3*, 2071.
(32) Grover, S., and Lawrence, C. B. (2017) The Alternaria alternata Mycotoxin Alternariol Suppresses Lipopolysaccharide-Induced Inflammation. *Int. J. Mol. Sci. 18*, 7.
(33) Berridge, M. V., Herst, P. M., and Tan, A. S. (2005) Tetrazolium dyes as tools in cell biology: new insights into their cellular reduction. *Biotechnol. Annu. Rev. 11*, 127−52.
(34) Christian, F., Smith, E. L., and Carmody, R. J. (2016) The Regulation of NF-κB Subunits by Phosphorylation. *Cells 5* (1), 12.
(35) Nakajima, S., and Kitamura, M. (2013) Bidirectional regulation of NF-kappaB by reactive oxygen species: a role of unfolded protein response. *Free Radical Biol. Med. 65*, 162−174.
(36) Li, Q., Chen, L., Dong, Z., Zhao, Y., Deng, H., Wu, J., Wu, X., and Li, W. (2019) Piperlongumine analogue L50377 induces pyroptosis via ROS mediated NF-κB suppression in non-small-cell lung cancer. *Chem.-Biol. Interact. 313*, 108820.
(37) Wakim, J., Goudenege, D., Perrot, R., Gueguen, N., Desquiret-Dumas, V., Chao de la Barca, J. M., Dalla Rosa, I., Manero, F., Le Mao, M., Chupin, S., Chevrollier, A., Procaccio, V., Bonneau, D., Logan, D. C., Reynier, P., Lenaers, G., and Khiati, S. (2017) CLUH couples mitochondrial distribution to the energetic and metabolic status. *J. Cell Sci. 130* (11), 1940−1951.
(38) de la Haba, C., Morros, A., Martinez, P., and Palacio, J. R. (2016) LPS-Induced Macrophage Activation and Plasma Membrane Fluidity Changes are Inhibited Under Oxidative Stress. *J. Membr. Biol. 249* (6), 789−800.
(39) de la Haba, C., Palacio, J. R., Martinez, P., and Morros, A. (2013) Effect of oxidative stress on plasma membrane fluidity of THP-1 induced macrophages. *Biochim. Biophys. Acta, Biomembr. 1828* (2), 357−64.
(40) Kiefel, H., Pfeifer, M., Bondong, S., Hazin, J., and Altevogt, P. (2011) Linking L1CAM-mediated signaling to NF-κB activation. *Trends Mol. Med. 17* (4), 178−187.
(41) Kiefel, H., Bondong, S., Erbe-Hoffmann, N., Hazin, J., Riedle, S., Wolf, J., Pfeifer, M., Arlt, A., Schäfer, H., Müerköster, S. S., and Altevogt, P. (2010) L1CAM−integrin interaction induces constitutive NF-κB activation in pancreatic adenocarcinoma cells by enhancing IL-1β expression. *Oncogene 29* (34), 4766−4778.
(42) Solhaug, A., Wisbech, C., Christoffersen, T. E., Hult, L. O., Lea, T., Eriksen, G. S., and Holme, J. A. (2015) The mycotoxin alternariol

induces DNA damage and modify macrophage phenotype and inflammatory responses. *Toxicol. Lett. 239* (1), 9−21.
(43) Solhaug, A., Torgersen, M. L., Holme, J. A., Lagadic-Gossmann, D., and Eriksen, G. S. (2014) Autophagy and senescence, stress responses induced by the DNA-damaging mycotoxin alternariol. *Toxicology 326*, 119−29.
(44) Schmutz, C., Cenk, E., and Marko, D. (2019) The Alternaria Mycotoxin Alternariol Triggers the Immune Response of IL-1beta-stimulated, Differentiated Caco-2 Cells. *Mol. Nutr. Food Res. 63*, e1900341.
(45) Hoesel, B., and Schmid, J. A. (2013) The complexity of NF-kappaB signaling in inflammation and cancer. *Mol. Cancer 12*, 86.
(46) Liu, T., Zhang, L., Joo, D., and Sun, S.-C. (2017) NF-κB signaling in inflammation. *Signal Transduction and Targeted Therapy 2* (1), 17023.
(47) Frattaruolo, L., Carullo, G., Brindisi, M., Mazzotta, S., Bellissimo, L., Rago, V., Curcio, R., Dolce, V., Aiello, F., and Cappello, A. R. (2019) Antioxidant and Anti-Inflammatory Activities of Flavanones from Glycyrrhiza glabra L. (licorice) Leaf Phytocomplexes: Identification of Licoflavanone as a Modulator of NF-kB/MAPK Pathway. *Antioxidants (Basel, Switzerland) 8* (6), 186.
(48) Somensi, N., Rabelo, T. K., Guimaraes, A. G., Quintans-Junior, L. J., de Souza Araujo, A. A., Moreira, J. C. F., and Gelain, D. P. (2019) Carvacrol suppresses LPS-induced pro-inflammatory activation in RAW 264.7 macrophages through ERK1/2 and NF-kB pathway. *Int. Immunopharmacol. 75*, 105743.
(49) Bao, L., Li, J., Zha, D., Zhang, L., Gao, P., Yao, T., and Wu, X. (2018) Chlorogenic acid prevents diabetic nephropathy by inhibiting oxidative stress and inflammation through modulation of the Nrf2/HO-1 and NF-kB pathways. *Int. Immunopharmacol. 54*, 245−253.
(50) Kang, S. Y., Shin, J. S., Kim, S. Y., Noh, Y. S., Lee, S. J., Hwang, H., Deyou, T., Jang, Y. P., and Lee, K. T. (2019) Caffeoyloxy-5,6-dihydro-4-methyl-(2H)-pyran-2-one isolated from the leaves of Olinia usambarensis attenuates LPS-induced inflammatory mediators by inactivating AP-1 and NF-kappaB. *Chem.-Biol. Interact. 309*, 108718.
(51) Li, X., Mu, P., Qiao, H., Wen, J., and Deng, Y. (2018) JNK-AKT-NF-kappaB controls P-glycoprotein expression to attenuate the cytotoxicity of deoxynivalenol in mammalian cells. *Biochem. Pharmacol. 156*, 120−134.
(52) Ying, C., Hong, W., Nianhui, Z., Chunlei, W., Kehe, H., and Cuiling, P. (2019) Nontoxic concentrations of OTA aggravate DON-induced intestinal barrier dysfunction in IPEC-J2 cells via activation of NF-kappaB signaling pathway. *Toxicol. Lett. 311*, 114−124.
(53) Kraus, K., Kleene, R., Braren, I., Loers, G., Lutz, D., and Schachner, M. (2018) A fragment of adhesion molecule L1 is imported into mitochondria and regulates mitochondrial metabolism and trafficking. *J. Cell Sci. 131*, jcs210500.
(54) Lingappan, K. (2018) NF-kappaB in Oxidative Stress. *Current opinion in toxicology 7*, 81−86.
(55) Haddad, J. J., Olver, R. E., and Land, S. C. (2000) Antioxidant/pro-oxidant equilibrium regulates HIF-1alpha and NF-kappa B redox sensitivity. Evidence for inhibition by glutathione oxidation in alveolar epithelial cells. *J. Biol. Chem. 275* (28), 21130−9.
(56) Muroya, T., Ihara, Y., Ikeda, S., Yasuoka, C., Miyahara, Y., Urata, Y., Kondo, T., and Kohno, S. (2003) Oxidative modulation of NF-kappaB signaling by oxidized low-density lipoprotein. *Biochem. Biophys. Res. Commun. 309* (4), 900−5.
(57) Kim, J. E., You, D. J., Lee, C., Ahn, C., Seong, J. Y., and Hwang, J. I. (2010) Suppression of NF-kappaB signaling by KEAP1 regulation of IKKbeta activity through autophagic degradation and inhibition of phosphorylation. *Cell. Signalling 22* (11), 1645−54.
(58) Murphy, M. P. (2009) How mitochondria produce reactive oxygen species. *Biochem. J. 417* (1), 1−13.
(59) de la Roche, M., Hamilton, C., Mortensen, R., Jeyaprakash, A. A., Ghosh, S., and Anand, P. K. (2018) Trafficking of cholesterol to the ER is required for NLRP3 inflammasome activation. *J. Cell Biol. 217* (10), 3560−3576.
(60) Desai, R., East, D. A., Hardy, L., Crosby, J., Rigon, M., Faccenda, D., Alvarez, M. S., Singh, A., Mainenti, M., Hussey, L. K., Bentham, R., Szabadkai, G., Zappulli, V., Dhoot, G., Romano, L. E., Dong, X., Hamechar-Brady, A., Chapple, J. P., Fleck, R. A., Vizcay-Barrena, G., Smith, K., and Campanella, M. Mitochondria form cholesterol tethered contact sites with the Nucleus to regulate retrograde response. (2019) *bioRxiv*, 445411, DOI: 10.1101/445411, version 2 https://www.biorxiv.org/content/10.1101/445411v2.full (accessed Jan 26, 2020).
(61) Quiros, P. M., Mottis, A., and Auwerx, J. (2016) Mitonuclear communication in homeostasis and stress. *Nat. Rev. Mol. Cell Biol. 17* (4), 213−26.